Ting-Ting Li[1, 2],
Xiayun Zhang[1],
Yunlong Wang[1],
Mengxuan Li[1],
Jia-Horng Lin[1,2,3,4,5,*]

Synergistic Effects of Plasma Treatment and Fabric Structure on Stab-Resistance Performances of STF/Aramid Composite Fabrics

[1] School of Textiles, Innovation Platform of Intelligent and Energy-Saving Textiles, Tianjin Polytechnic University, Tianjin 300387, China

[2] Minjiang University, Department of Chemistry and Chemical Engineering, Fujian 350108, China

[3] Feng Chia University, Department of Fibre and Composite Materials, Laboratory of Fibre Application and Manufacturing, Taichung 40724, Taiwan,
* e-mail: jhlin@fcu.edu.tw

[4] China Medical University, School of Chinese Medicine, Taichung 40402, Taiwan

[5] Asia University, Department of Fashion Design, Taichung 41354, Taiwan

DOI: 10.5604/01.3001.0013.7318

Abstract
In order to improve the contribution of STF and fabric to the stab resistance of STF-impregnated aramid soft armour materials, the plasma treatment of various fabric structures was conducted. This study explored the interactive effects of plasma treatment, fabric structure and particle size on the spike and knife resistance properties of plasma-treated STF/Aramid fabrics. Fumed silica and polyethylene glycol (PEG) based STFs were prepared with various particle sizes (15 nm, 75 nm) at a solid content of 15%. Various weave structures of fabrics (plain, 2/2 twill, 5/3 satin, 2/2 basket) were impregnated with STF and then plasma-treatment conducted. The rheological behaviour of STF in various silica sizes as well as the spike and knife quasi-static stab resistances of the resultant plasma-treated STF/aramid fabrics in various weave structures were both explored. The results show that the various weave structures of STF/Aramid fabrics treated with plasma exhibited a significant enhancement of quasi-static spike resistance. Furthermor, 2/2 twill, 5/3 satin and basket weaving plasma -treated STF/Aramid with a coarser silica particle in STF showed a higher improvement in quasi-static spike resistance. Interactive effect results show that the plasma treatment of fabric and the silica size in STF affected spike resistance more significantly, while knife resistance was only significantly affected by the fabric structure.

Key words: *aramid fibre, weaving, stab resistance, shear thickening fluid, plasma treatment.*

Introduction

Woven aramid fabrics are used to provide protection against sharp-pointed weapons in soft body armour due to their soft and flexible structure [1]. Conventional body armour requires multiple layers of aramid fabrics, which makes it inflexible and bulky in application [2]. Shear thickening fluid (STF) has the significant benefit of reducing the number of layers in stab resistance protection. STF is a non-Newtonian flow fluid which consists of rigid particles and a dispersion medium. This smart fluid exhibits a colloidal suspension in a normal state, but increases in viscosity under applied loadings, presenting a solid-like state. After removing the loading applied to the medium, the fluid returns to a liquid state [3-5].

Recently, many studies have been conducted on the impact resistance of STF-impregnated aramid fabrics. Decker et al. [6] and Hassan et al. [7] reported that the stab resistances of STF-treated fabrics exhibited a significant improvement over neat fabric with an equivalent areal weight. For better understanding of the effect of medium and particle characteristics on the stab resistance protection of STF-treated fabrics, some studies have been carried out by researchers. Kalman et al. [8] examined the effect of particle hardness on the spike puncture behaviour of fabrics intercalated with STF, and showed that SiO_2-based STF had a better spike resistance than PMMA-based STF. Gong et al. [9] studied the effects of dispersing particles and the medium on drop-tower knife and spike resistance, and indicated that silica-based STF exhibited the highest knife stab resistance. Furthermore, the shape of the silica particle affected the rheological behaviour of STF, and it was demonstrated that fumed silica-based STF exhibits rapid thickening behavior in comparison to colloidal silica-based STF. Thus, the stab resistance of soft armour can be improved at a lower solid content by using fumed silica [10]. According to these studies, fumed silica in STF possessed excellent knife and spike stab resistance due to increasing the friction between yarns.

In order to investigate fabric response against quasi-static low-velocity impact loading, Lu et al [11] impregnated STF into warp-knitted spacer fabric (WKSF). It is indicated that WKSF/STF composites can be used as damping materials under impact loading. Messiry and Eltahan [12] compared the stab resistance properties of triaxial woven fabrics as well as woven and knitted fabrics and showed that Vectran triaxial weave fabrics can be designed to enhance stab performance. Majumdar and Laha [13, 14] investigated the effect of the weaving structure on yarn pulling-out and the impact properties of STF-impregnated fabrics and found that plain weave fabrics before and after STF-treatment had the highest pulling-out force, and that the enhancement of the weaving structure in impact energy absorption after STF impregnation was opposite to that before STF. These findings were different to the results by Chua et al. that structures like 2/2 basket and satin facilitate high energy absorption [15], and that satin and plain weaves were best for ballistic protection application, as indicated by Shimek and Fahrenthold [16]. Unlike these studies, we systemically focused on the effects of weaving structures and silica size on the spike and knife resistance of STF/aramid fabrics. Furthermore, concepts of plasma-treatment to improve the stab resistances of STF/aramid fabrics were proposed which can provide a reference for designing flexible and high-performance stab-resisting soft body armours. This study provides a substitute for the fabric layers in our previous designs of flexible stab-resisting composite fabrics [17-19] which can reduce the number of layers and area weight in soft armour application.

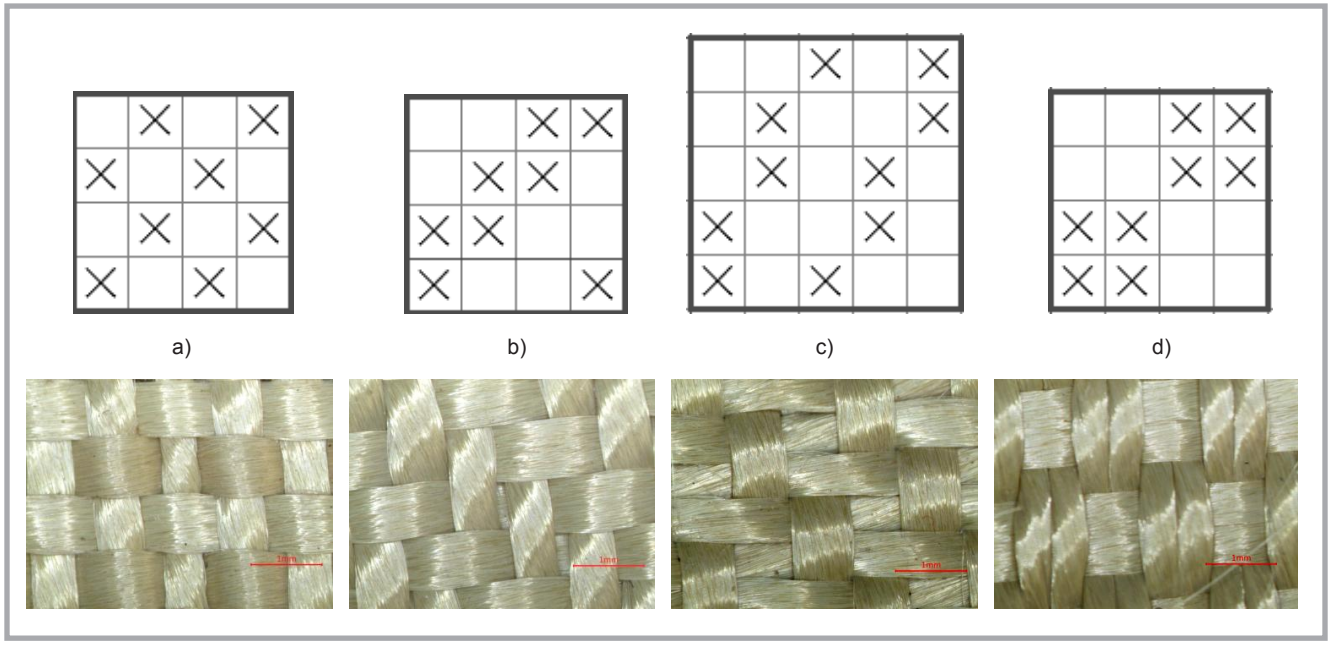

Figure 1. *Four kinds of weaving pattern of aramid fabrics: a) plain weave, b) 2/2 twill weave, c) 5/3 satin weave, d) 2/2 basket weave.*

Material and methods

Materials

The high-performance fabrics used in this study were made from Aramid 1414 strands supplied by Sinopec Yizheng Chemical Fibre Co. Ltd, China, whose fineness was 112 tex/500f, tenacity – 128.9 N and breaking elongation – 2.49%. The STF was based on fumed silica which had a particle size of 15 nm and 75 nm, provided by Guangzhou GBS high-tech & Industry Co. Ltd., China. The liquid medium was Polyethylene glycol (PEG) 200, purchased from the Tianjin Xingfu Fine Chemical Research Institute, China.

Table 1. *Parameters of the four weaves of aramid fabrics.*

Pattern	Warp density /(/10cm)	Weft density /(/10cm)	Cross-point number /(/cm^2)	Area weight /(g/m^2)	Thickness /mm
Basket Weave (B)	130	205	75	408.02	0.732
Plain Weave (P)	130	115	52	280.52	0.482
Twill Weave (T)	130	160	42	325.93	0.521
Satin Weave (S)	130	160	33	347.86	0.586

Table 2. *Physical parameters of STF-treated aramid and plasma-treated STF/aramid fabrics.*

Name code	Warp density /(/10 cm)	Weft density /(/10 cm)	Area weight /(g/m^2)
15 nm STF-B	130	210	565.00
15 nm STF-P	130	110	404.12
15 nm STF-T	130	160	484.36
15 nm STF-S	130	160	521.24
PT-15 nm STF-B	130	210	573.12
PT-15 nm STF-P	130	110	464.40
PT-15 nm STF-T	130	160	509.47
PT-15 nm STF-S	130	160	527.35
75 nm STF-B	130	210	655.40
75 nm STF-P	130	110	434.40
75 nm STF-T	130	160	538.09
75 nm STF-S	130	160	557.58
PT-75 nm STF-B	130	210	703.16
PT-75 nm STF-P	130	110	479.24
PT-75 nm STF-T	130	160	582.91
PT-75 nm STF-S	130	160	593.68

STF preparation and treatment of composite fabrics

In order to discuss the influence of the fabric structure on the stab resistance of aramid fabrics, four weaving patterns were designed. Aramid 1414 strands were preliminary twisted at 200 turns/m for the clean weaving followed. The twisted stands were then woven with different weaving constitutions (see ***Figure 1***), using a loom, to fabricate Plain (P), Twill (T), Satin (S) and Basket (B) weaves of Aramid fabrics. The structures of the fabrics are displayed in Figure 2. Physical parameters of the fabricated aramid fabrics are shown in ***Table 1***. The plain, twill, satin and basket weaves of aramid fabrics were abbreviated as fabrics P, T, S and B.

In the STF preparation, various particle sizes of fumed silica (15 nm and 75 nm) as a dispersion phase were dispersed into a PEG 200 medium using a mechanical stirrer at 300 rpm for 2 hrs and ultrasonic oscillation at 200 Hz for 30 min to fabricate 15 nm and 75 nm STF suspensions. A low amount of fumed silica was combined with PEG repeatedly until there was a solid content of 15% for the homogeneous STF suspension system after three times circulation of mechanical stirring and ultrasonic oscillations.

For the STF/Aramid fabrics, pure aramid fabrics were first plasma processed at 120 Pa and 100 W for 60 s to increase the roughness of the surface of the com-

posite fabrics. The treated fabrics were impregnated into 15 nm and 75 nm STF suspension systems using an ultrasonic vibration meter (Changzhou Xinren Ultrasonic Equipment Co., LTD) for 120 min. The impregnated STF/Aramid fabrics were pressed at 625 Pa, and then dried at 80 °C for 2 hrs using a DZF-6050 Vacuum Drying Oven (Shanghai Xinyin medical machine Co., LTD). All sample codes and specifications of the STF-treated aramid fabrics and plasma-treated STF/aramid fabrics are revealed in ***Table 2***. Therein, 15 nm STF-B is the 15 nm STF-impregnated basket-weave aramid fabric, and PT-15 nm STF-B is the plasma-treated basket-weave STF/Aramid fabric.

Measurements and characterisation

Rheological behaviour test

Rheological tests were performed using an Autosorb-1C rheometer (Malvern Instruments, UK) with 40 mm diameter parallel plate apparatus. The gap between the plates was kept at 2 mm, and the shear rate was increased from 1 to 1000 s^{-1}. The measurement was completed at a temperature of 25 °C.

Flexibility test

The flexibility of STF/Aramid fabrics was tested by the incline method with a slope angle of 45° (see ***Figure 2***). Fabrics pressed by a steel rule were placed on a platform, and then pushed ahead slowly until the fabric edge touched the incline. The rectangular fabric was of 200 mm length and 25 mm width. The forward distance of the steel rule showed the bending length (LB), which was used to characterise the flexibility of the fabrics. The flexural rigidity (B, cN·cm^2/cm) was calculated using ***Equation (1)***.

$$B = 9.81 \times 10^{-8} \times W \times LB \qquad (1)$$

Where, W was the weight per unit area, g/m^2.

Tensile test

The tensile strength of STF/Aramid fabrics was tested in accordance with ASTM D5035-11. An Instron 5566 universal testing machine (Instron, USA) was used to measure rectangular specimens. The crosshead speed was 200 mm/min, and the tensile specimen was 180 mm long and 25.4 mm wide.

Quasi-static stab resistance test

According to ASTM 1342-05, different weave structures of STF/aramid fabrics were tested by an Instron 3369 (Instron, USA). Two heads (spike and knife) were attached to the load cell and then penetrated into the samples, clamped between the plates, at a constant velocity. The penetrated speed was 508 mm/min. The testing heads' dimensions are displayed in ***Figure 3***. The instrument can record the compression load-displacement curves. The maximum compression load shows the maximum static stab resistance.

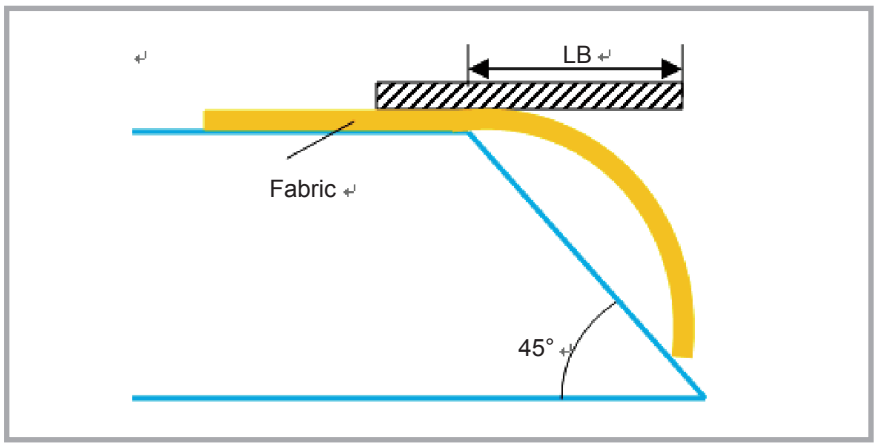

Figure 2. *Schematic representation of flexibility test.*

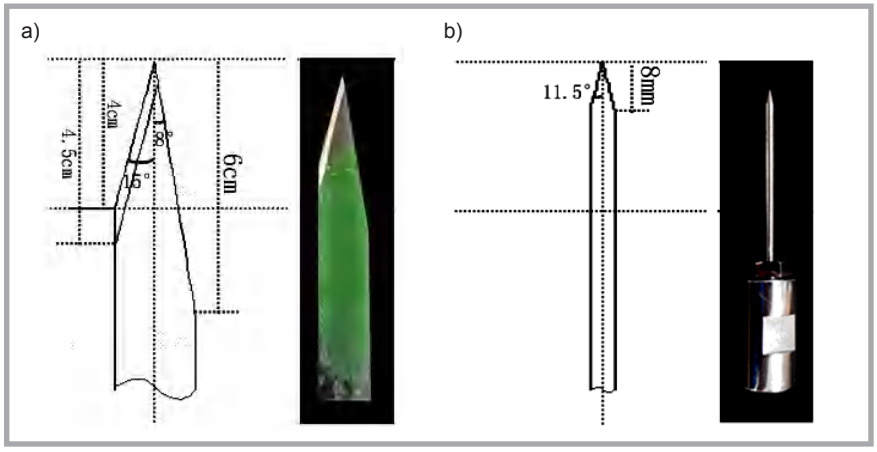

Figure 3. *Geometric shapes of knife and spike heads: a) knife head, b) spike head.*

Results and discussion

Rheological behaviour of STF

Figure 4 shows the viscosity of STF in relation to the steady shear rate. It is found that at different fumed silica particle sizes, shear thinning and shear thickening behaviors are observed. The viscosity of STF firstly decreases, then increases to the maximum, and finally decreases. It shows that firstly the STF

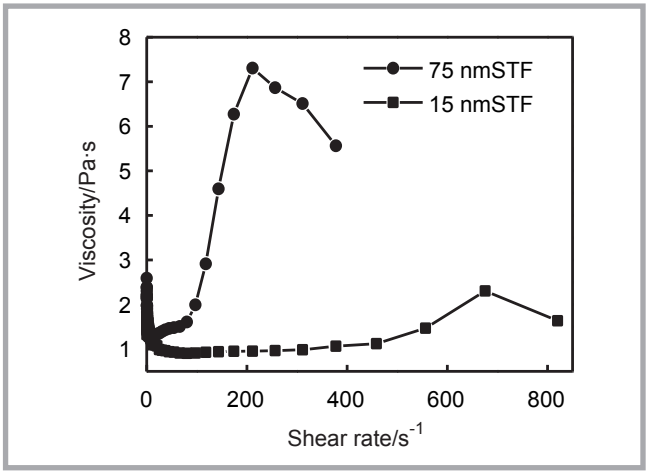

Figure 4. *Rheological behaviour of STF with various silica particle sizes.*

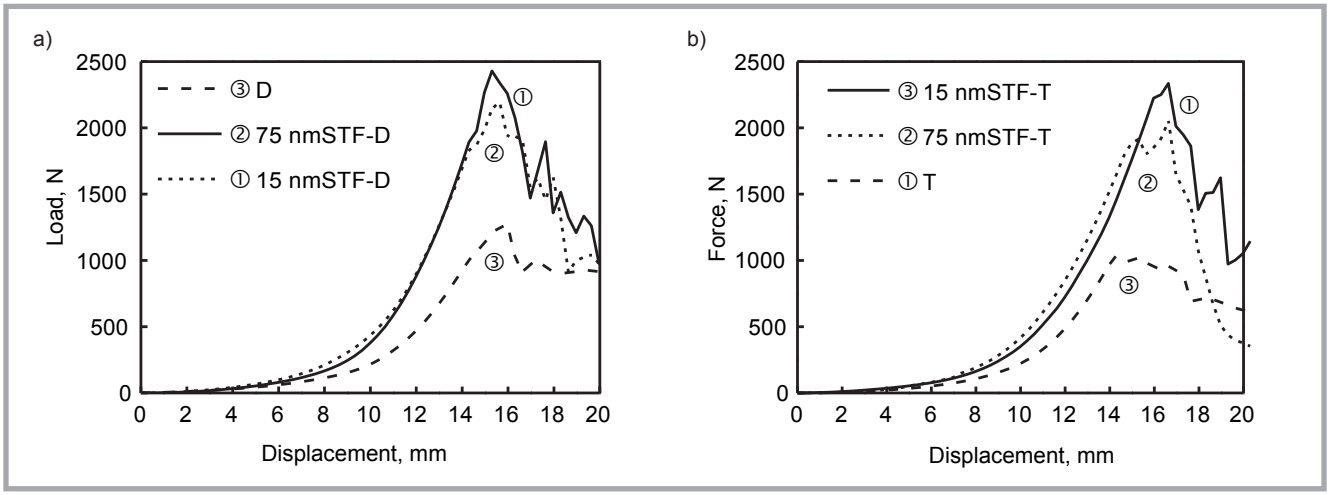

Figure 5. *Tensile behaviors of STF-impregnated aramid fabrics with: a) satin weave and b) twill weave.*

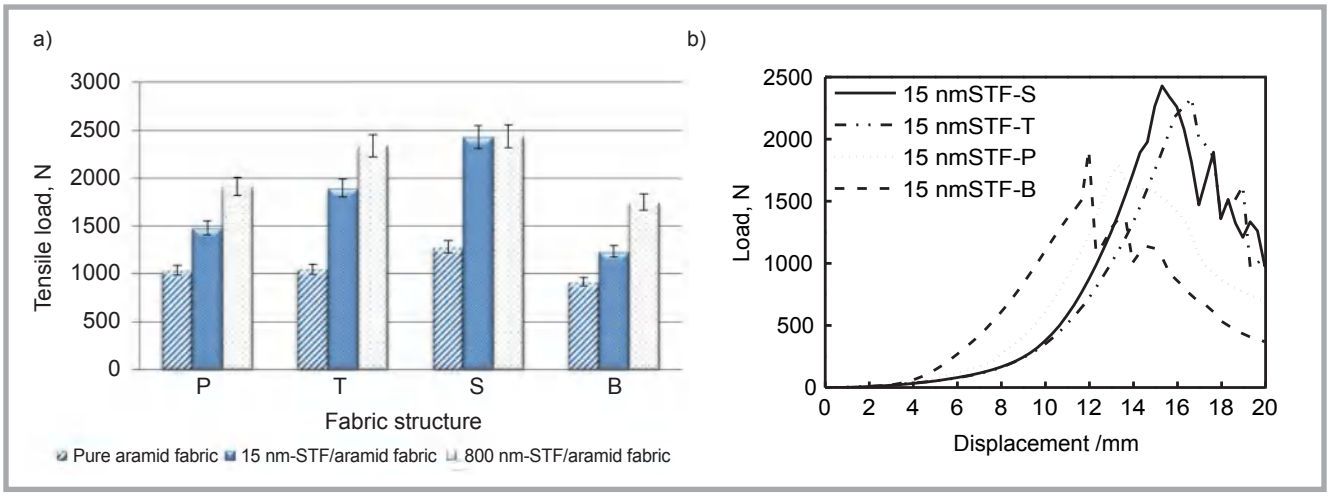

Figure 6. *a) Maximum tensile forces of pure aramid STF / fabrics with various particles, and b) tensile curves of 75 nm STF-impregnated aramid fabrics with various fabric structures.*

underwent shear thinning, then shear thickening, and finally secondary shear thinning after removing the loading applied. The thickening mechanism can be explained by the hydrocluster theory, which is based on particle interactions in a liquid medium [3, 4]. On the basis of this, the hydrodynamic force induces the formation of particle clusters. Hydrodynamic interaction dominates the suspension at low shear rates due to the contactless rheology, but under higher shear rates, particles contact with each other, and therefore clusters are formed due to Brownian forces [20]. Once the hydroclusters are formed, the average length between the aggregates and Brownian times increases. By increasing the shear rate, the cluster tends to break up and the distance between particles decreases at a higher shear rate, forming orthokinetic aggregation when hydrodynamic interactions become predominant [3].

Furthermore, with an increasing particle size, the rheological behaviors become more significant, and the critical shear rate shifts to a lower value. The critical shear rate decreases from 80 s^{-1} to 17 s^{-1} when the silica particle increases from 15 nm to 75 nm, and the maximum viscosity increases from 0.91 Pa·s to 1.3 Pa·s correspondingly. This finding is consistent with the results indicated by Hasanzadeh, Lee and Srivastava et al., namely that an increase in silica particle size from 100 to 500 nm significantly decreases the critical shear rate [3, 4, 21].

Tensile property of STF/aramid fabrics

Figure 5 shows the tensile behaviours of pure aramid and STF/aramid fabrics with a satin-and twill weave. It is found that the aramid fabric after STF impregnation exhibited a much higher maximum tensile force, which is because STF significantly enhanced the inter-yarn friction of the fabric as confirmed by yarn pull-out studies [2, 9, 13, 22]. Furthermore, the silica size affected the tensile property significantly; and aramid fabric immersed with coarser silica in STF exhibited a higher maximum tensile force, reaching 90.6% and 122.8% for the satin and twill weave structures, respectively. As seen in ***Figure 6.a***, even with plain and 2/2 basket, the bigger silica in STF still showed a larger enhancement. This finding is not associated with the result found by Lee et al. [21] that smaller particles exhibited the largest increment in inter-yarn friction, which is due to different weight add-on percentages on fabrics among the various particle sizes.

Comparing the different weave structures of the fabrics, the 5/3 satin weave showed the highest maximum tensile force, followed by the 2/2 twill, plain, and 2/2 bas-

ket weaves, as displayed in ***Figure 6.a***. Being impregnated into STF, the satin and twill weave aramid fabrics possessed the best tensile property compared to the plain and basket weaves. The 5/3 satin weave has the maximum weft density and longest floating length (see ***Figure 1*** and ***Table 1***), which contributes to the STF impregnation amounts and increases the inter-yarn friction. However, even the basket weave has the same floating length and higher weft density with a twill weave, with the former exhibiting the lowest maximum tensile force. This difference can be explained by the complicated effects of crossover points and STF add-on amounts on thetensile property, as shown in ***Figure 6.b***, which displays the various tensile behaviors with different weave structures.

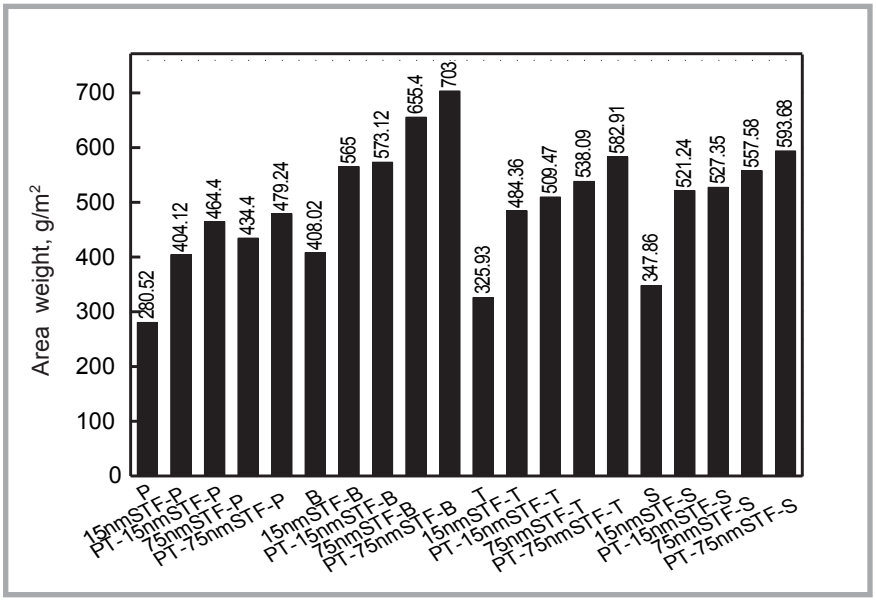

Figure 7. *Areal weights of pure aramid, STF/aramid and plasma-treated STF/aramid fabrics.*

Add-on amounts of STF on fabrics

Figure 7 shows the add-on amounts of STF for STF/aramid fabrics and plasma-treated STF/aramid fabrics. Comparatively, 75 nm silica particles can be impregnated into aramid fabrics higher than 15 nm silica??? regardless of the weave structure, which can explain the tensile property results in ***Figures 5*** and ***6***. As seen for the satin weave, for example, the STF amount is 173.38 g/m^2 after 15 nm-STF impregnation;, and that value increases to 209.72 g/m^2 when 75 nm silica particles are dispersed into the STF. For a plain structure, the STF amount is lower, reaching 123.6 (15 nm-STF) and 153 (75 nm-STF), respectively. It is because a higher crossover point density acts against the immersion of STF between yarns, but it is positively associated with pull-out forces and then impact energy [13, 14], which shows that the fabric structure and STF impregnation have a complicated effect on impact resistance.

Furthermore, plasma treatment is conducive to increasing the impregnation amounts of STF in fabric fibres, regardless of the structure of the fabric. The enhancement of STF amounts by plasma treatment reached 1.2%-14.9% for 15 nm-silica and 6.5%-10.3% for 75 nm-silica. Conversely, plasma treatment improved the plain structure most significantly. This is because oxygen plasma treatment introduced some new polar groups (O – C = O) on the fibre surface, increased the fibre surface roughness by plasma etching and oxidative reactions and then increased the specific surface area of fibres, and improved the coupling bonding and adsorption capacity of aramid fibres for STF [23-26].

The surface of untreated and plasma-treated STF/aramid fabrics was observed by scanning electron microscope (TM 3030, Hitach Ltd, Japan). As seen in ***Figure 8***, it is found that STF impregnation on the fibre surface treated with plasma is obviously higher than for untreated STF/aramid fabrics. Comparing ***Figure 8.b*** and ***Figure 8.c***, the STF amount at crossover points becomes higher \ \, and ***Figure 7*** confirms that plasma-treatment for the plain structure is more obvious????.

Stab resistances of STF/aramid fabrics

As mentioned above, different structures became impregnated with various STF amounts, resulting in a changed areal weight. Spike and knife resistances also depend on the areal weight, as mentioned in our previous study [27]. Therefore, the normalised values of spike and knife resistances were used for an unbiased comparison of results. Normalisation was made using the following ***Equation (2)***.

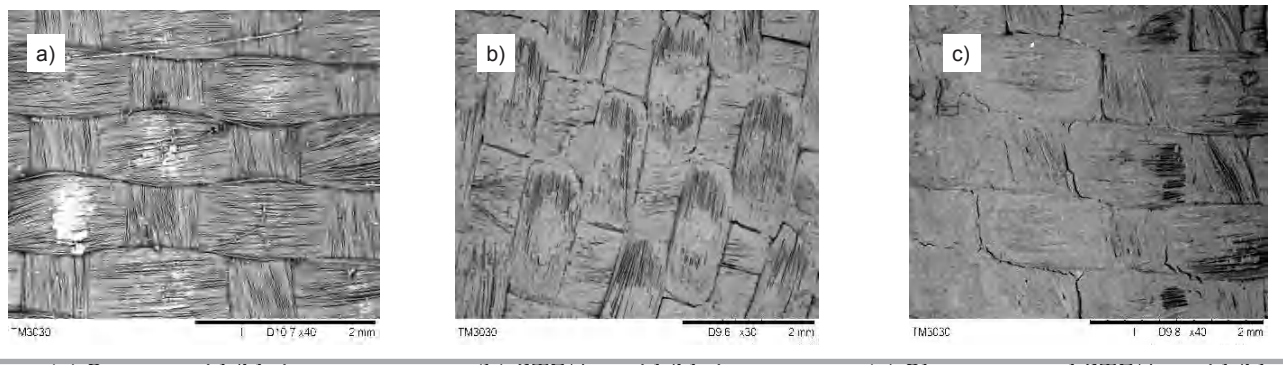

Figure 8. *SEM observations of aramid, STF/aramid and plasma-treated STF/Aramid fabric: a) pure aramid fabric, b) STF/Aramid fabric, c) plasma-treated STF/Aramid fabric.*

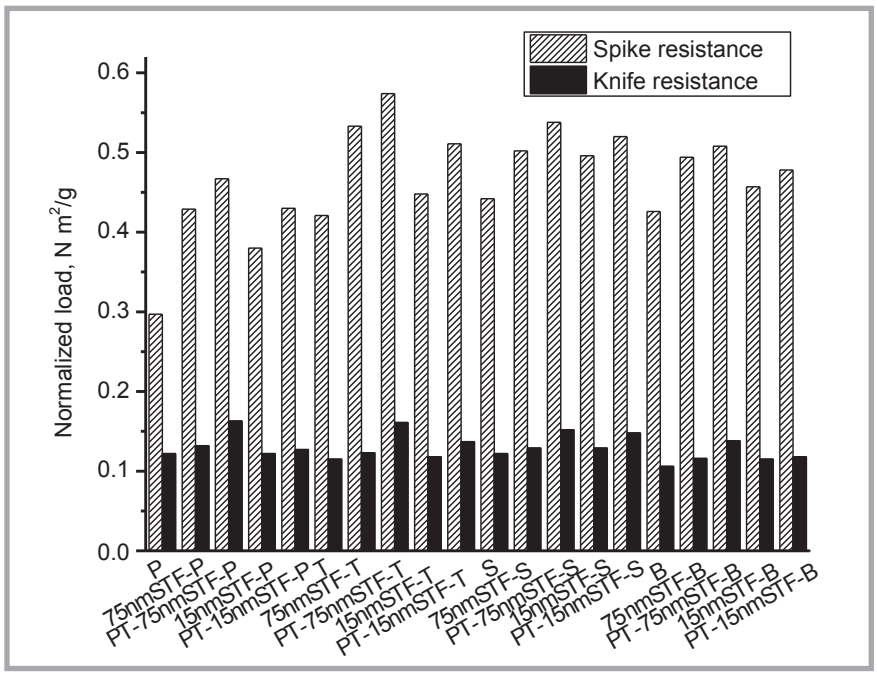

Figure 9. *Normalised knife and spike resistances of pure aramid, STF/aramid and plasma-treated STF/aramid fabrics with various weave structures and silica sizes.*

$$F_N = \frac{F}{A} \tag{2}$$

Where, F_N is the normalised spike and knife resistance, F – the maximum spike and knife resistance force, and A is the areal weight, g/m^2.

The normalised spike and knife resistances of pure aramid, STF/aramid and plasma-treated STF/aramid fabrics are shown in ***Figure 9***. STF impregnation evidently improved both the spike and stab resistance whatever the fabric structure. This is because of two factors: The first is when STF/aramid fabrics were penetrated at speed of 508 mm/min, the STF underwent shear-thickening behavior that transformed from the liquid state to a solid state, which absolutely enhanced the spike and knife resistance force [7]. The second is that STF can increase the interactions of yarns and filaments, which restricts the mobility of

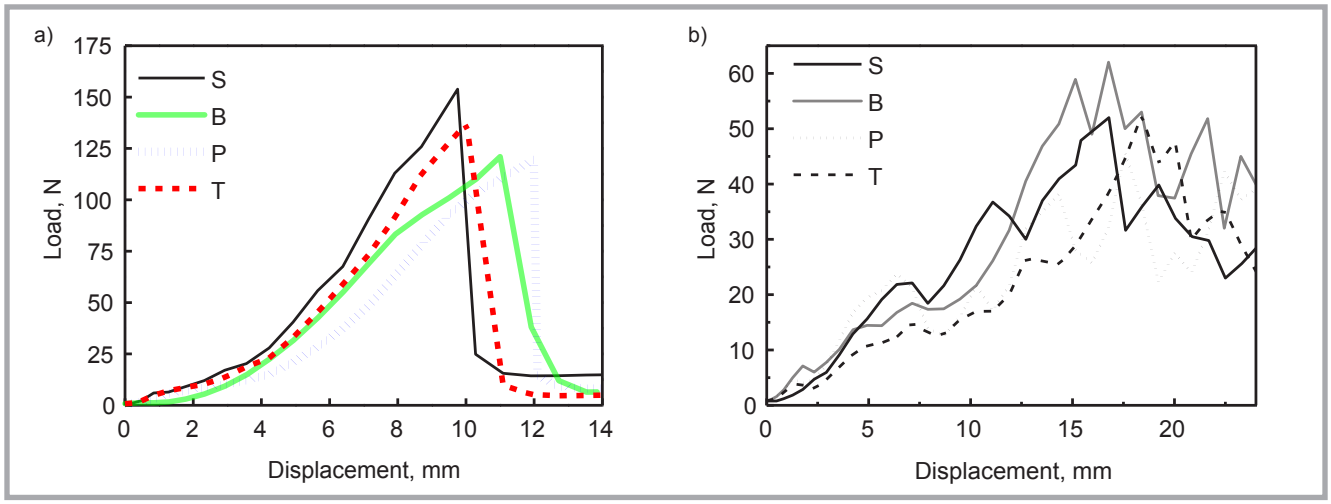

Figure 10. *a) Spike resistance and knife resistance, b) behaviours of fabrics with various structures.*

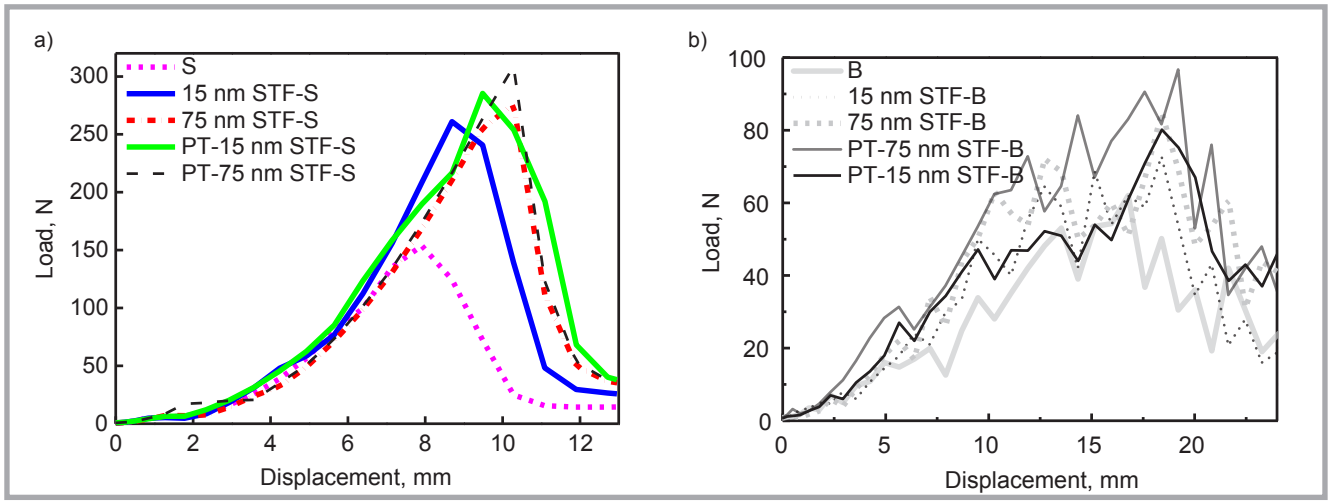

Figure 12. *a) Spike resistances of STF/aramid and plasma-treated STF/aramid fabrics with a satin structure and various particles sizes, b) knife resistances of STF/aramid and plasma-treated fabrics with a basket structure and various particles sizes.*

yarns and filaments, making it difficult for the spike and knife to separate filaments [2]. Furthermore, the bigger silica particles in STF had higher spike and knife resistances, attributed to the fact that bigger silica particles have a smaller critical shear rate and higher viscosity at a lower shear rate, making the inter-yarn friction stronger and the stab resistance property higher [3-4].

Spike and knife resistance behaviours of the different structures of fabrics are displayed in ***Figure 10.a*** and ***10.b***. In an untreated condition, 5/3 satin weave woven fabrics showed the highest spike resistance, followed by the 2/2 twill weave, basket weave and plain weave. Interlacement points caused stress concentration, as indicated in our study, thus puncture stress transferred loads along yarns difficultly, which weakened the spike resistance [28]. However, the 2/2 basket weave exhibited a knife resistance consistent with the high-velocity impact resistance results [15, 29]. The two differences in spike and knife stab resistance of the fabric structure is due to the fracture mechanisms.

As seen in ***Figure 11.a***, the damage to the fabric caused by a spike stab was dominated by yarn separation, and only a small part of the fibre was fractured due to STF impregnation. ***Figure 11.b*** shows that after knife stab penetration, cut fracture of the yarn and separation between yarns were found at the damage surface. The yarn firstly separated when the knife point penetrated into the fabrics, and then was cut when the knife blade contacted the yarn. Yarn fracture played the main role in knife stab failures.

As displayed in ***Figures 9*** and ***12***, plasma treatment improved the spike and knife stab resistance of STF/aramid regardless of fabric structures and silica size in the STF. It is because when the plasma attacked the surface of the aramid fibres, free radicals could be generated on their surface and the surface of fibres became activated.; meanwhile, the fibre surface was etched, the roughness increased, and then the wettability of the fibres improved. Based on the physical-chemical effects on the aramid fibres, the chemical bonds and mechanical interlocking between aramid fibres and STF were enhanced, which increased the STF impregnation amount and reinforced the stab resistance [23, 24].

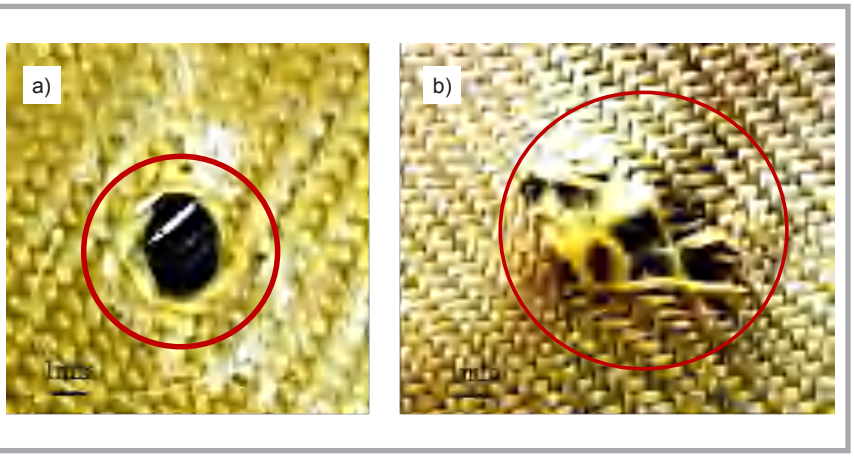

Figure 11. *Failure observations of STF/aramid fabrics a) after a spike and b) knife stab.*

Table 3. *ANOVA analysis of spike and knife resistance results.*

ANOVA analysis of spike resistance					
Source	**Type III sum of squares**	**df**	**Mean square**	**F**	**Sig.**
Corrected model	182758.772[a]	19	9618.883	4.568	.000
Intercept	2993509.784	1	2993509.784	1421.642	.000
Fabric structure	21507.451	3	7169.150	3.405	.027
Plasma treatment	13965.796	1	13965.796	6.632	.014
SiO_2 size	75206.903	2	37603.451	17.858	.000
Fabric * SiO_2	12904.233	6	2150.706	1.021	.426
Plasma * SiO_2	288.504	1	288.504	.137	.713
Fabric * plasma	754.018	3	251.339	.119	.948
Fabric * plasma * SiO_2	1103.653	3	367.884	.175	.913
Error	82121.156	39	2105.671		
Total	3546495.688	59			
Corrected total	264879.928	58			
a. R^2 = .690 (adjusted R^2 = .539)					
ANOVA analysis of knife resistance					
Source	**Type III sum of squares**	**df**	**Mean square**	**F**	**Sig.**
Corrected model	6187.462[a]	19	325.656	2.586	.019
Intercept	155137.657	1	155137.657	1231.987	.000
Fabric structure	3329.743	3	1109.914	8.814	.001
SiO_2 size	846.890	2	423.445	3.363	.054
Plasma treatment	196.671	1	196.671	1.562	.225
Fabric * plasma	238.545	3	79.515	.631	.603
Plasma * SiO_2	20.273	1	20.273	.161	.692
Fabric * plasma * SiO_2	16.735	3	5.578	.044	.987
Fabric * SiO_2	856.242	6	142.707	1.133	.378
Error	2644.419	21	125.925		
Total	175300.668	41			
Corrected total	8831.881	40			
a. R^2 = .701 (adjusted R^2 = .430)					

Especially, the spike resistance of basket weaving fabric after STF treatment is increased by 106% (75 mm silica) and 100.5% (15 nm silica). Basket and satin weaves impregnated with 75 nm STF have a more significant improvement in knife resistance than the other fabric structures, which is due to the STF amounts between yarns in various fabric structures. Plasma treatment played the biggest role in the basket weave, with the improvement of spike stab resistance after plasma treatment reaching 56 N (75 nm-STF) and 34 N (15 nm-STF), while that of knife resistance was only 5-15 N, as compared to untreated STF fabrics. This implies that the effects of plasma treatment, silica size and fabric structure on spike and knife resistances are different. Therefore, ANOVA analy-

Table 4. *Flexibility of STF/aramid fabrics.*

Name codes	Flexible length L_B, mm	Area weight *W*, g/m^2	Flexibility ridigity, cN·cm^2/cm	Standard deviation σ
P	118	280.52	45.2	0.96
B	111	408.02	60.5	0.70
T	87	325.93	21.1	1.10
S	98	347.86	32.1	0.79
75 nmSTF-P	91	434.4	32.1	0.81
75 nmSTF-B	98	655.4	54.7	0.78
75 nmSTF-T	74	538.09	21.4	0.59
75 nmSTF-S	83	557.58	31.3	0.93
15 nmSTF-P	82	404.12	21.9	0.77
15 nmSTF-B	101	565	57.1	0.58
15 nmSTF-T	77	484.36	21.7	0.72
15 nmSTF-S	84	521.24	30.3	1.02

ses of spike and knife resistances were conducted using SPSS software, shown in ***Table 3***. It can be found that three processing parameters: silica size, fabric structure and plasma treatment all affect spike resistance significantly at a confidence level of 95%; therein the silica size had the most significant influence, followed by plasma treatment and fabric structure. However, a significance analysis of knife resistance results showed that only the fabric structure affected the knife resistance significantly at a confidence level of 95%. The different processing parameters influencing spike and knife stab resistances can be verified by the mechanisms of stab damage, as reported in ***Figure 11***.

Flexibility of composite fabric

Table 4 shows the flexural length and flexural rigidity of pure aramid and STF/Aramid fabrics. As ***Equation (1)*** proves, the flexural property of the fabrics depends on the flexural length and area weight. That is, the longer the flexural length and the bigger the area weight were, the bigger the flexural rigidity was. A bigger flexural rigidity demonstrates that the fabric is hard to bend, hence the lower softness. As seen in ***Table 4***, STF impregnation tends to decrease the flexural rigidity, which is because the STF soaked between fibres, acting as lubrication, and thus increasing the fabric softness. Comparatively, the twill and satin woven aramid fabrics have a softer texture regardless of the impregnation of 15 nm and 75 nm silica particles because both of them have a relatively higher floating length and lower crossover points, as confirmed in ***Figure 1***; which demonstrates that twill and satin-weave fabrics can produce softer STF-impregnated body armours.

Conclusions

In this study, plasma treatment and weave structure were both designed to improve STF-impregnated fabrics. The interactive influences of plasma treatment and fabric structure on the stab-resistance performances of STF/aramid soft armour materials were discussed. Rheological behaviour results of STF showed that coarser silica particles exhibited more significant shear thickening behaviour. The critical shear rate decreases from 80 s^{-1} to 17 s^{-1} when the silica particle is increased from 15 nm to 75 nm, and the maximum viscosity increases from 0.91 Pa·s to 1.3 Pa·s correspondingly. The significant shear-thickening coarser silica in STF improved the tensile, spike and knife resistances. Moreover, STF impregnation reduced the flexural rigidity due to lubrication effects from STF on yarns. Plasma treatment increased STF amounts significantly, regardless of the weave structure of the fabrics, and also improved the spike and knife resistance at the per unit areal weight. Its enhancement for a spike and knife is different, with the former being larger than the latter. The main damage mechanism for spike resistance is yarn separation, and for knife resistance it is the cut fracture of the yarn. The plasma treatment increased the yarn fracture due to the increment in inter-yarn friction. Interactive effects showed that the silica size and plasma treatment affected the spike resistance more significantly, while only the fabric structure significantly affected the knife resistance. Therefore, an appropriate combination of the STF characteristic and fabric structure after plasma-treatment can effectively eliminate the number of layers of soft armour, thus providing a novel direction for designing more flexible and lightweight soft armour. This study only focuses on the interactive effects on quasi-static stab resistance, and in the following study we will place more emphasis on the influence of plasma-treatment on the drop-tower stab resistance of STF/aramid fabrics.

Acknowledgements

This work was supported by the National Natural Science Foundation of China (NSFC 51503145, 11702187) and the Opening Project of Green Dyeing and Finishing Engineering Research Center of Min Jiang University.

References

1. Feng X, Li S, Wang Y, Wang Y, Liu J. Effects of Different Silica Particles on Quasi-Static Stab Resistant Properties of Fabrics Impregnated with Shear Thickening Fluids. *Materials & Design* 2014; 64: 456-61.
2. Gürgen S, Kuşhan MC. The Stab Resistance of Fabrics Impregnated with Shear Thickening Fluids Including Various Particle Size of Additives. *Composites Part A-Applied Science and Manufacturing* 2017; 94, 50-60.
3. Hasanzadeh M, Mottaghitalab V. The Role of Shear-Thickening Fluids (STFs) in Ballistic and Stab-Resistance Improvement of Flexible Armor. *Journal of Materials Engineering and Performance* 2014; 23, 4: 1182-1196.
4. Srivastava A, Majumdar A, Butola BS. Improving The Impact Resistance of Textile Structures by Using Shear Thickening Fluids: A Review. *Critical Reviews in Solid State and Materials Sciences* 2012; 37, 2: 115-29.
5. Barnes HA, Shear-Thickening ("Dilatancy") in Suspensions of Nonaggregating Solid Particles Dispersed in Newtonian Liquids. *Journal of Rheology* 1989; 33: 329-366.
6. Decker MJ, Halbach CJ, Nam CH, Wagner NJ, Wetzel ED. Stab Resistance of Shear Thickening Fluid (STF)-Treated Fabrics. *Composites Science and Technology* 2007; 67, 3: 565-578.
7. Hassan TA, Rangari VK, Jeelani S. Synthesis, Processing and Characterization of Shear Thickening Fluid (STF) Impregnated Fabric Composites. *Materials Science and Engineering A-Structural Materials Properties Microstructure and Processing* 2010; 527, 12: 2892-2899.
8. Kalman DP, Merrill RL, Wagner NJ, Wetzel ED. Effect of Particle Hardness on the Penetration Behavior of Fabrics Intercalated with Dry Particles and Concentrated Particle-Fluid Suspensions. *ACS Applied Materials & Interfaces* 2009; 1, 11: 2602-2612.
9. Gong X, Xu Y, Zhu W, Xuan S, Jiang W, Jiang W. Study of the Knife Stab and Puncture-Resistant Performance

for Shear Thickening Fluid Enhanced Fabric. *Journal of Composite Materials* 2014; 48, 6: 641-657.
10. Kang TJ, Kim CY, Hong KH. Rheological Behavior of Concentrated Silica Suspension and its Application to Soft Armor. *Journal of Applied Polymer Science* 2012; 124, 2: 1534-1541.
11. Lu Z, Wu L, Gu B, Sun B. Numerical Simulation of the Impact Behaviors of Shear Thickening Fluid Impregnated Warp-Knitted Spacer Fabric. *Composites Part B-Engineerin*g 2015; 69: 191-200.
12. Messiry El M, Eltahan E. Stab Resistance of Triaxial Woven Fabrics for Soft Body Armor. *Journal of Industrial Textiles* 2016; 45, 5: 1062-1082.
13. Majumdar A, Laha A. Effects of Fabric Construction and Shear Thickening Fluid on Yarn Pull-Out From High-Performance Fabrics. *Textile Research Journal* 2016; 86, 19: 2056-2066.
14. Laha A, Majumdar A. Interactive Effects of P-Aramid Fabric Structure and Shear Thickening Fluid on Impact Resistance Performance of Soft Armor Materials. *Materials & Design* 2016; 89: 286-293.
15. Chua CK, Chena YL. Ballistic-Proof Effects of Various Woven Constructions. *FIBRES & TEXTILES in Eastern Europe* 2010; 18, 6 (83): 83-87.
16. Shimek ME, Fahrenthold EP. Effects of Weave Type on the Ballistic Performance of Fabrics. *AIAA Journal* 2012; 50, 11: 2558-2565.
17. Li TT, Wang R, Lou CW, Lin JH. Static and Dynamic Puncture Behaviors of Compound Fabrics with Recycled High -Performance Kevlar Fibres. *Composites Part B-Engineering* 2014; 59: 60-66.
18. Li TT, Wang R, Lou CW, Lin JY, Lin JH. Static and Dynamic Puncture Failure Behaviors of 3D Needle-Punched Compound Fabric Based on Weibull Distribution, *Textile Research Journal* 2014; 84, 18:1903-1914.
19. Li TT, Lou CW, Lin JY, Lin MC, Lin JH. Static and Dynamic Puncture Properties of Intra-/Inter-Laminar Reinforced Multilayer Compound Fabrics by Needle-Punching and Thermal Bonding. *Textile Research Journal* 2016; 86, 14: 1487-1497.
20. Peters IR, Majumdar S, Jaeger HM. Direct Observation of Dynamic Shear Jamming in Dense Suspensions. *Nature* 2016; 532, 7598: 214-217.
21. Lee BW, Kim IJ, Kim CG. The Influence Of The Particle Size of Silica on The Ballistic Performance of Fabrics Impregnated with Silica Colloidal Suspension. *Journal of Composite Materials* 2009; 43, 23: 2679-2698.
22. Srivastava A, Majumdar A, Butola BS. Improving The Impact Resistance Performance of Kevlar Fabrics using Silica Based Shear Thickening Fluid. *Materials Science and Engineering A-Structural Materials Properties Microstructure and Processing* 2011; 529: 224-229.
23. Wang J, Chen P, Li H, Li W, Wang B, Zhang C, Ni R. Surface Characteristic of Poly (P-Phenylene Terephthalamide). *Fibres with Oxygen Plasma Treatment, Surface and Interface Analysis* 2008; 40, 9: 1299-1303.
24. Ren Y, Wang C, Qiu Y. Influence of Aramid Fibre Moisture Regain During Atmospheric Plasma Treatment on Aging of Treatment Effects on Surface Wettability and Bonding Strength to Epoxy. *Applied Surface Science* 2007; 253, 23: 9283-9289.
25. On SY, Kim MS, Kim SS. Effects of Post-Treatment of Meta-Aramid Nanofibre Mats on The Adhesion Strength of Epoxy Adhesive Joints. *Composite Structures* 2017; 159: 636-645.
26. Martinez MA, Abenojar J, Enciso B, Velasco FJ. Effect of Atmospheric Plasma Torch on Ballistic Woven Aramid. *Textile Research Journal*, 0040517516671122, 2016.
27. Li TT, Wang R, Lou CW, Huang CH, Lin JH. Mechanical and Physical Properties of Puncture-Resistance Plank Made of Recycled Selvages. *Fibres and Polymers* 2013; 14, 2: 258-265.
28. Li TT, Fang J, Huang CH, Lou CW, Lin JY, Lin MC, Lin JH. Numerical Simulation of Dynamic Puncture Behaviors of Woven Fabrics Based on the Finite Element Method. *Textile Research Journal* 2017; 87, 11: 1308-1317.
29. Hosur MV, Vaidya UK, Ulven C, Jeelani S. Performance of Stitched/Unstitched Woven Carbon/Epoxy Composites under High Velocity Impact Loading. *Composite Structures* 2004; 64, 3: 455-466.

Received 06.11.2017 Reviewed 20.11.2017